EXPLAINING EXTREME EVENTS OF 2016

From A Climate Perspective

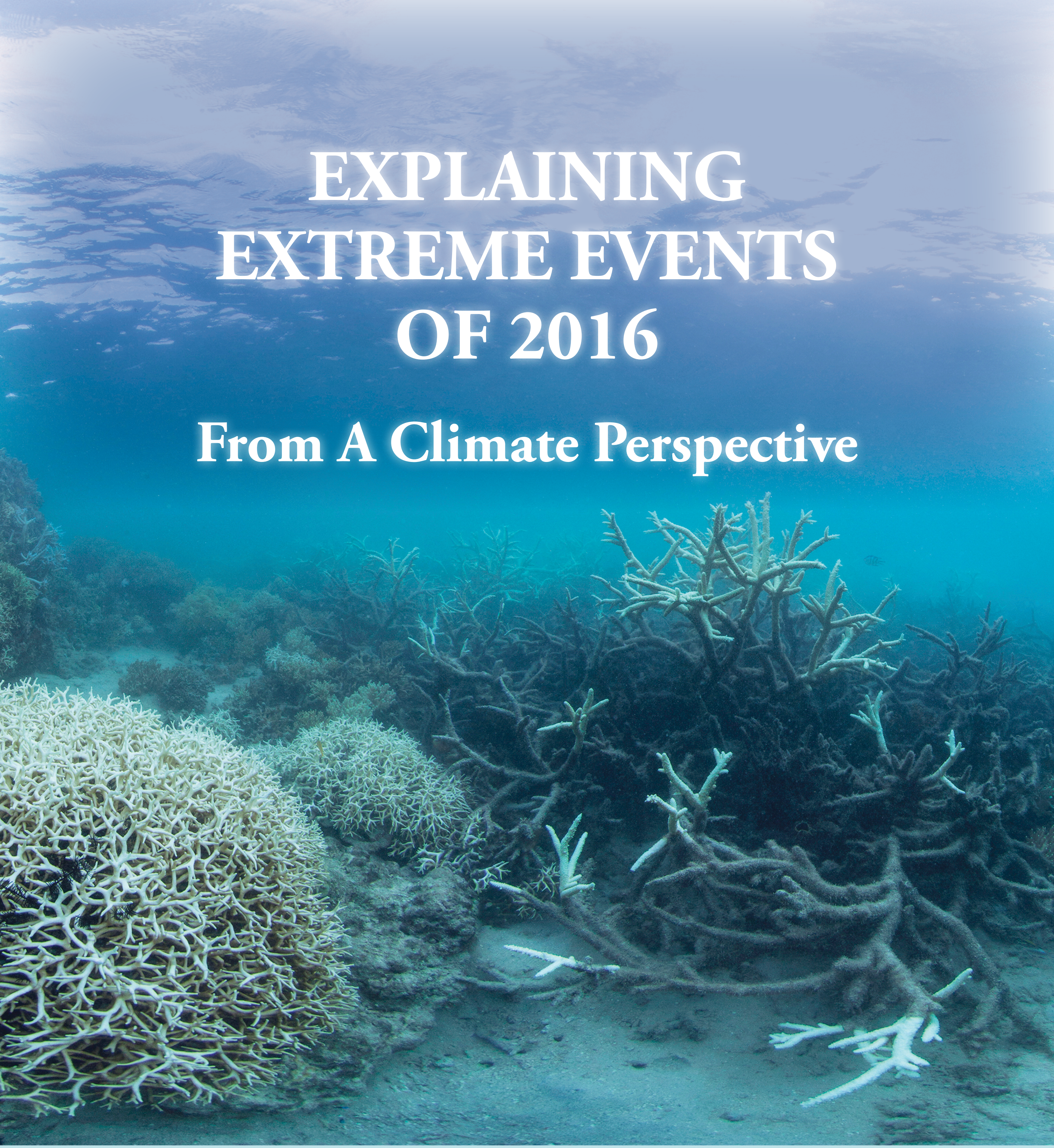

Special Supplement to the
Bulletin of the American Meteorological Society
Vol. 99, No. 1, January 2018

EXPLAINING EXTREME EVENTS OF 2016 FROM A CLIMATE PERSPECTIVE

Editors

Stephanie C. Herring, Nikolaos Christidis, Andrew Hoell, James P. Kossin,
Carl J. Schreck III, and Peter A. Stott

Special Supplement to the

Bulletin of the American Meteorological Society

Vol. 99, No. 1, January 2018

American Meteorological Society

Corresponding Editor:

Stephanie C. Herring, PhD
NOAA National Centers for Environmental Information
325 Broadway, E/CC23, Rm 1B-131
Boulder, CO 80305-3328
E-mail: stephanie.herring@noaa.gov

Cover credit:

©The Ocean Agency / XL Catlin Seaview Survey / Chrisophe Bailhache—A panoramic image of coral bleaching at Lizard Island on the Great Barrier Reef, captured by The Ocean Agency / XL Catlin Seaview Survey / Christophe Bailhache in March 2016.

HOW TO CITE THIS DOCUMENT

Citing the complete report:

Herring, S. C., N. Christidis, A. Hoell, J. P. Kossin, C. J. Schreck III, and P. A. Stott, Eds., 2018: Explaining Extreme Events of 2016 from a Climate Perspective. *Bull. Amer. Meteor. Soc.*, **99** (1), S1–S157.

Citing a section (example):

Quan, X.W., M. Hoerling, L. Smith, J. Perlwitz, T. Zhang, A. Hoell, K. Wolter, and J. Eischeid, 2018: Extreme California Rains During Winter 2015/16: A Change in El Niño Teleconnection? [in "Explaining Extreme Events of 2016 from a Climate Perspective"]. *Bull. Amer. Meteor. Soc.*, **99** (1), S54–S59, doi:10.1175/BAMS-D-17-0118.1.

EDITORIAL AND PRODUCTION TEAM

Riddle, Deborah B., Lead Graphics Production, NOAA/NESDIS National Centers for Environmental Information, Asheville, NC

Love-Brotak, S. Elizabeth, Graphics Support, NOAA/NESDIS National Centers for Environmental Information, Asheville, NC

Veasey, Sara W., Visual Communications Team Lead, NOAA/NESDIS National Centers for Environmental Information, Asheville, NC

Fulford, Jennifer, Editorial Support, Telesolv Consulting LLC, NOAA/NESDIS National Centers for Environmental Information, Asheville, NC

Griffin, Jessicca, Graphics Support, Cooperative Institute for Climate and Satellites-NC, North Carolina State University, Asheville, NC

Misch, Deborah J., Graphics Support, Telesolv Consulting LLC, NOAA/NESDIS National Centers for Environmental Information, Asheville, NC

Osborne, Susan, Editorial Support, Telesolv Consulting LLC, NOAA/NESDIS National Centers for Environmental Information, Asheville, NC

Sprain, Mara, Editorial Support, LAC Group, NOAA/NESDIS National Centers for Environmental Information, Asheville, NC

Young, Teresa, Graphics Support, Telesolv Consulting LLC, NOAA/NESDIS National Centers for Environmental Information, Asheville, NC

TABLE OF CONTENTS

ABSTRACT—Stephanie C. Herring, Nikolaos Christidi, Andrew Hoell, James P. Kossin, Carl J. Schreck III, and Peter A. Stott

This sixth edition of explaining extreme events of the previous year (2016) from a climate perspective is the first of these reports to find that some extreme events were not possible in a preindustrial climate. The events were the 2016 record global heat, the heat across Asia, as well as a marine heat wave off the coast of Alaska. While these results are novel, they were not unexpected. Climate attribution scientists have been predicting that eventually the influence of human-caused climate change would become sufficiently strong as to push events beyond the bounds of natural variability alone. It was also predicted that we would first observe this phenomenon for heat events where the climate change influence is most pronounced. Additional retrospective analysis will reveal if, in fact, these are the first events of their kind or were simply some of the first to be discovered.

Last year, the editors emphasized the need for additional papers in the area of "impacts attribution" that investigate whether climate change's influence on the extreme event can subsequently be directly tied to a change in risk of the socio-economic or environmental impacts. Several papers in this year's report address this challenge, including Great Barrier Reef bleaching, living marine resources in the Pacific, and ecosystem productivity on the Iberian Peninsula. This is an increase over the number of impact attribution papers than in the past, and are hopefully a sign that research in this area will continue to expand in the future.

Other extreme weather event types in this year's edition include ocean heat waves, forest fires, snow storms, and frost, as well as heavy precipitation, drought, and extreme heat and cold events over land. There were a number of marine heat waves examined in this year's report, and all but one found a role for climate change in increasing the severity of the events. While human-caused climate change caused China's cold winter to be less likely, it did not influence U.S. storm Jonas which hit the mid-Atlantic in winter 2016.

As in past years, the papers submitted to this report are selected prior to knowing the final results of whether human-caused climate change influenced the event. The editors have and will continue to support the publication of papers that find no role for human-caused climate change because of their scientific value in both assessing attribution methodologies and in enhancing our understanding of how climate change is, and is not, impacting extremes. In this report, twenty-one of the twenty-seven papers in this edition identified climate change as a significant driver of an event, while six did not. Of the 131 papers now examined in this report over the last six years, approximately 65% have identified a role for climate change, while about 35% have not found an appreciable effect.

Looking ahead, we hope to continue to see improvements in how we assess the influence of human-induced climate change on extremes and the continued inclusion of stakeholder needs to inform the growth of the field and how the results can be applied in decision making. While it represents a considerable challenge to provide robust results that are clearly communicated for stakeholders to use as part of their decision-making processes, these annual reports are increasingly showing their potential to help meet such growing needs.

3. CMIP5 MODEL-BASED ASSESSMENT OF ANTHROPOGENIC INFLUENCE ON RECORD GLOBAL WARMTH DURING 2016

Thomas R. Knutson, Jonghun Kam, Fanrong Zeng, and Andrew T. Wittenberg

According to CMIP5 simulations, the 2016 record global warmth was only possible due to substantial centennial-scale anthropogenic warming. Natural variability made a smaller contribution to the January–December 2016 annual-mean global temperature anomaly.

Global annual-mean surface temperature set a record high in 2016 in at least three observational datasets—GISTEMP (Hansen et al. 2010), HadCRUT4.5 (Morice et al. 2012), and NOAA (Karl et al. 2015)—exceeding the previous record set in 2015 (Fig. 3.1a). In contrast, the last global mean annual *cold* record occurred around 1910. Record global warmth implies some record warmth on regional scales as well (Kam et al. 2016), which can cause important impacts such as thermal stress, coral bleaching, and melting of sea and land ice (IPCC 2013). Decreased land ice, combined with ocean heat uptake, contributes to sea level rise, which can exacerbate coastal flooding extremes (e.g., Lin et al. 2016).

Figure 3.1 compares observed global-mean temperature anomalies with simulations from the Coupled Model Intercomparison Project 5 (CMIP5; Taylor et al. 2012; Table ES3.1). Record warmth in 2016 largely follows a pronounced century-scale warming trend, and was far outside the range of internal (unforced) climate variability sampled across over 24 000 years of CMIP5 Control simulations (Fig. 3.1c). It was also well outside the range of CMIP5 Natural Forcing-Only simulations incorporating solar and volcanic forcing changes (Fig. 3.1b). In contrast, the observed warming lies within the range of CMIP5 All-Forcing simulations that include both anthropogenic and natural forcing (Fig. 3.1a). These results suggest that observed global-mean temperatures emerged from the natural variability background (natural forcing response plus internal variability) around 1980, and have become increasingly detectable since.

The inconsistency of observed long-term global warming with simulated natural variability (detection), and its consistency with simulations incorporating anthropogenic forcing (attribution), are in agreement with previous studies and assessments (e.g., IPCC 2001, 2007, 2013; Knutson et al. 2013; Kam et al. 2016). Detection and attribution of human influence on global mean temperature is well-established in the climate sciences, including through more sophisticated approaches than shown here (e.g., regressions or pattern scaling; Bindoff et al. 2013 and references therein). The adequacy of CMIP5 model simulations of internal variability for detection and attribution has also been assessed previously (e.g., IPCC 2013; Knutson et al. 2013, 2016).

Figure 3.1d examines shorter term global-mean temperature variability since 1970, highlighting the timing of four major El Niño events and two major volcanic eruptions. The 2015/16 global temperature event appears as a temporary bump with a magnitude (for January–December 2016) of a little over 0.1°C, superimposed on a long-term warming trend of about 1°C—the latter being largely attributable to anthropogenic forcing according to CMIP5 models (Figs. 3.1a,b). While the El Niño events of 1972/73, 1997/98, and 2015/2016 have apparent warming signatures in global temperature, the 1982/83 event's imprint was apparently muted by the almost-coincident eruption of El Chichón.

Monthly maps of observed surface temperature internal climate variability for 2016 are discussed in the online supplement material. From these and previous studies (e.g., Trenberth et al. 2002) we infer that the short-term calendar-year global mean warmth in 2015 and 2016 is likely to have been at least partly

AFFILIATIONS: Knutson, Zeng, and Wittenberg—NOAA/Geophysical Fluid Dynamics Laboratory, Princeton, New Jersey; Kam—Department of Civil, Construction, and Environmental Engineering, University of Alabama, Tuscaloosa, Alabama, and Cooperative Institute for Climate Science, Princeton University, Princeton, New Jersey

DOI:10.1175/BAMS-D-17-0104.1

A supplement to this article is available online (10.1175/BAMS-D-17-0104.2)

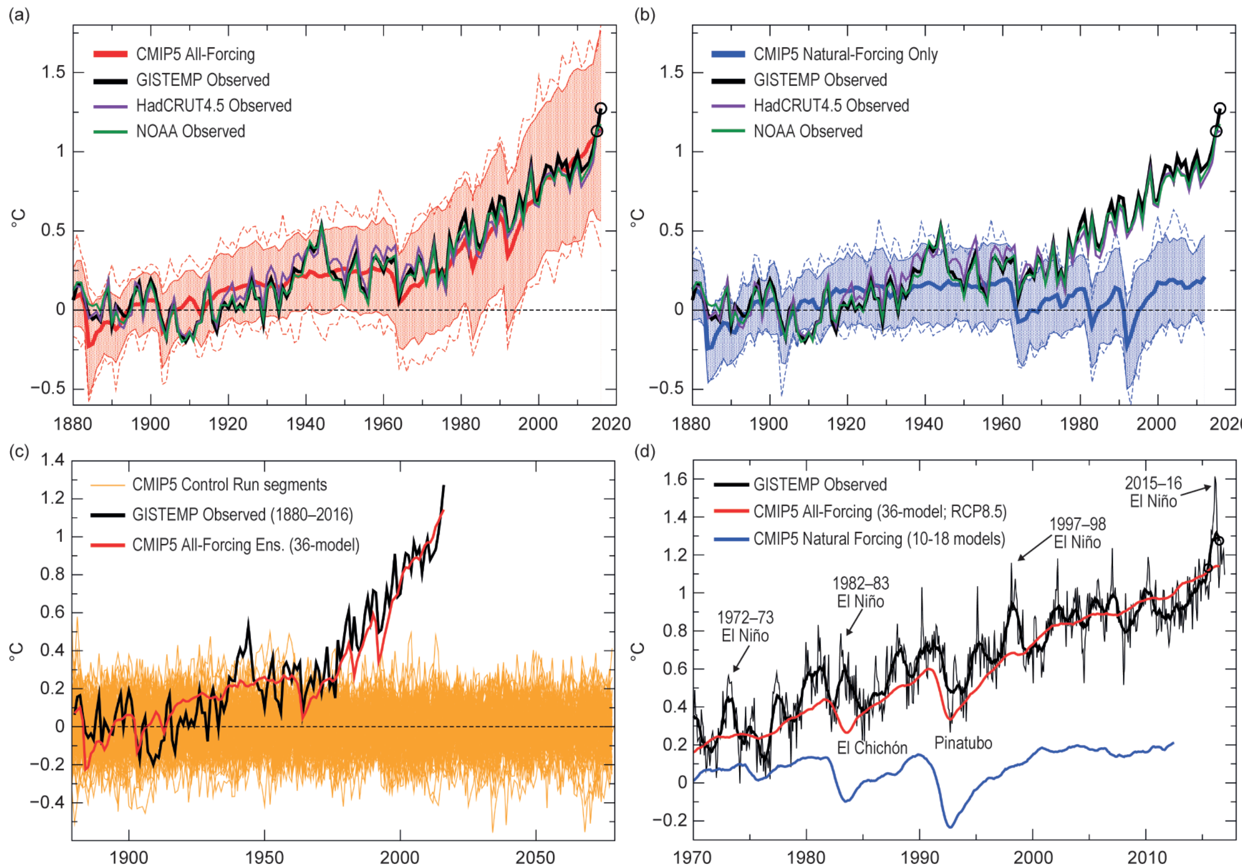

Fig. 3.1. Observed global-mean temperature anomalies vs. CMIP5 simulations (°C; 1881–1920 reference period). (a) CMIP5 All-Forcing (anthropogenic plus natural forcing) grand ensemble mean of individual ensemble means from 36 models (thick red curve); ±2 std. dev. (red shading) and minimum–maximum spread (dashed red) of annual means across individual simulations; and observed GISTEMP (black), HadCRUT4.5 (purple) and NOAA (green) anomalies. (b) As in (a) but for natural forcings (18 models; blue curves and shading). (c) Observed (GISTEMP; black) and All-Forcing grand ensemble mean (red) anomalies compared to 200-year segments from 36 CMIP5 control runs (orange). (d) 12-month running mean anomalies for GISTEMP observations (thick black; monthly anomalies are thin black) and CMIP5 All-Forcing (red) and Natural Forcing (blue) grand ensemble means. GISTEMP observed annual means (Jan–Dec) for 2015 and 2016 are highlighted by circles in panels (a), (b), and (d). See also online supplement materials.

El Niño-driven. Note that a calendar-year average generally leads to some cancellation between El Niño and the subsequent La Niña, since ENSO's equatorial Pacific SST anomalies tend to peak near the end of the calendar year, and its effect on global-mean temperature peaks a few months later.

For event attribution, we estimate the occurrence rate of annual-mean global temperature anomalies reaching 2015 or 2016 observed levels for simulated climates with and without anthropogenic forcing. Figure 3.2 explores the upper limits of simulated natural variability contributions to 2015 and 2016 global temperature. It depicts the maximum internal variability anomalies (from long control runs) and the Natural and Anthropogenic Forcing ensemble 2016 responses. Results are shown for each of seven CMIP5 models having at least two ensemble members each for the Natural-Forcing, All-Forcing, and RCP8.5 scenarios (the latter are needed for extending All-Forcing to 2016). Within this framework, the anthropogenic contribution dominates over the Natural Forcing and potential internal variability contributions. Figure 3.2 shows the ensemble-mean and most- and least-conservative estimates (see caption), across the models, of the natural + internal variability contribution to 2016's anomaly. None of the CMIP5 models produce natural + internal variability large enough to reproduce the observed 2015 and 2016 extremes—even using very long control simulations (in one case 5200 years). We therefore conclude that, according to the CMIP5 simulations, 2015- or 2016-level warmth (relative to the ~1900 baseline) never occurs without

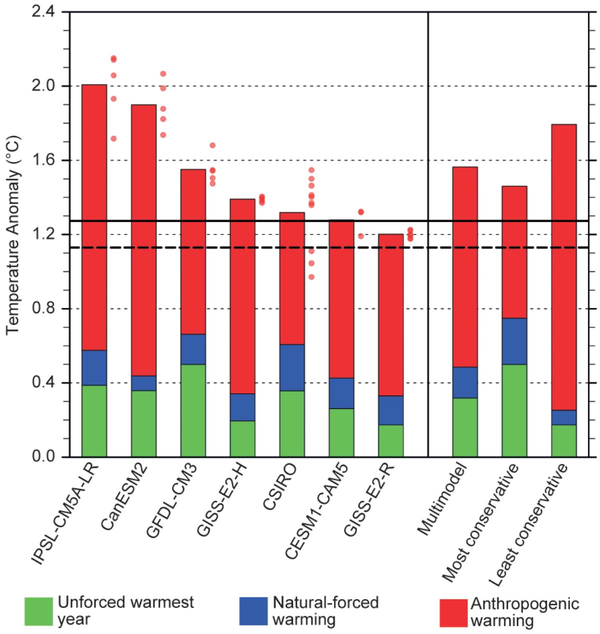

Fig. 3.2. Observed 2015 (dashed black line) and 2016 (solid) global mean temperature anomalies (°C, relative to 1881–1920) vs. simulated 2016 anomalies from the seven CMIP5 models having multiple All-Forcing/RCP8.5 and Natural Forcing ensemble members. Each model's largest positive internal variability anomaly (green) is combined with that model's ensemble mean Natural- (blue) or Anthropogenic-forcing (red, computed as All-Forcing minus Natural-Forcing) response. The "Multimodel" estimate uses the grand ensemble mean of ensemble means of the Natural and Anthropogenic responses along with the average of the maximum positive internal variability anomalies of the individual models. The "Most conservative" combines the largest internal and Natural Forcing contributions, from any model, with the smallest anthropogenic contribution. The "Least conservative" combines the smallest maximum internal and smallest natural forcing, from any of model, with the largest anthropogenic contribution.

anthropogenic forcing, and is only possible with anthropogenic forcing.

Estimated contributions from different forcing sets to the 2016 observed global mean anomaly (1.27°C)—with internal variability computed as a residual—are presented in Table ES3.1 for each model. Using all 36 CMIP5 models, the mean estimated internal variability residual for 2016 was 0.12°C (10% of the total 2016 anomaly relative to 1881–1920). For the 12 models having at least two All-Forcing and RCP8.5 scenario members, the internal variability estimate was 0.09°C (7%). For the seven of twelve models that also passed a consistency test for 2011 and 2016 (online supplement material), the internal variability mean (and range) were 0.14°C (–0.14° to +0.31°C), that is, 11% (–11% to +24%). There were also seven models having at least two ensemble members each for All-Forcing, RCP8.5, and Natural Forcing scenarios; their ensemble-mean contributions were 1.04°C (82%) from Anthropogenic Forcing, and 0.16°C (13%) from Natural-Forcing. Using only the four of these seven models that also passed the consistency test, the mean and range of contributions across the models were 0.88°C (69%), with range 0.71° to 1.05 °C (56% to 83%) for Anthropogenic Forcing, and 0.18°C (14%) with range 0.15° to 0.25°C (12% to 20%) for Natural Forcing.

The margins of error for some of our assessments are also illustrated in Fig. 3.2. Using each of seven models' ensemble Natural Forcing response estimates, the internal variability in these models would need to be 2.2 to 6.4 (1.9 to 5.6) times larger than simulated for the Natural Forcing plus internal variability alone to reach the 2016 (2015) observed value, even given the model's most extreme internal event. For example, for GFDL-CM3, the Natural-Forcing estimate for 2016 is +0.16°C and the model's strongest internal variability event (0.50°C) would need to be multiplied by 2.22 to reach the observed anomaly level (1.27°C). Alternatively, using each model's most extreme internal variability event, the Natural Forcing mean response from the models would need to be 3.6 to 11 (3.1 to 9.7) times larger than simulated to match the observed temperature anomalies for 2016 (2015).

The fraction of attributable risk (FAR) is defined as FAR = 1 – (p_0/p_1), where p_0 is the modeled probability of the event in a climate without anthropogenic influence, and p_1 is the probability in a climate with anthropogenic influence (Stott et al. 2004). For the CMIP5 models, we have already shown that $p_0 \sim 0$; that is, an event like 2015 or 2016 appears to be essentially impossible under the available estimates of natural forcings, without including anthropogenic forcings. However, events as warm as 2016 are clearly possible in at least some of the All-Forcing experiments with anthropogenic forcing (Fig. 3.1a). We therefore estimated ensemble and individual model p_1's, for the seven models having more than one All-Forcing/RCP8.5 ensemble member and that also passed the consistency test (online supplement material); ensemble p_1 was estimated from the grand ensemble mean and the aggregate distribution of annual anomalies from the individual control runs. The estimated p_1 for exceeding the 2015 (2016) observed threshold is 0.86 (0.42), implying a return period of only 1.2 (2.4) years. However, these return time estimates are highly uncertain, as they depend on (uncertain) estimates of the All-Forcing response for 2015 and 2016; even in this case where we exclude inconsistent CMIP5 models, the return time for the 2016 threshold ranges from 1 to 39 years. We have not attempted to estimate return times for cases where the event is outside the modeled distribution, or for the observations directly (with 2016 being the single most extreme event in the observed distribution). We conclude that for the seven individual CMIP5 models having adequate numbers of ensemble members and having All-Forcing runs that are consistent with recent observations, the risk of exceeding the 2015 (2016) threshold is entirely attributable to anthropogenic forcing (FAR = 1).

Our analysis has important caveats. The internal variability of the climate system and the response to historical forcings have been estimated here using a combination of observations and models following Knutson et al. (2013, 2016). Uncertainties also remain in historical climate forcings by various agents, including anthropogenic aerosols. However, simulated internal variability would need to be more than twice as large as the most extreme case found in the CMIP5 models, for even the most extreme simulated natural warming event to match the 2016 observed record.

Summary. According to the CMIP5 simulations, 2016's record global January–December warmth would not have been possible under climate conditions of the early 1900s—anthropogenic forcing was a necessary condition (Hannart et al. 2016) for the event. Anthropogenic forcing contributed most of this warmth (relative to 1881–1920 conditions), while natural forcings and intrinsic variability (including El Niño) made relatively small contributions to the January–December 2016 global mean.

ACKNOWLEDGMENTS. We thank the WCRP's Working Group on Coupled Modeling, and participating CMIP5 modeling groups, for making available the CMIP5 data; and the Hadley Centre, University of East Anglia Climatic Research Unit, NASS/GISS, and NOAA/NCEI for providing observational datasets. This study was partly funded by NOAA grant NA14OAR4320106.

REFERENCES

Bindoff, N. L., and Coauthors, 2013: Detection and attribution of climate change: From global to regional. *Climate Change 2013: The Physical Science Basis*, T. F. Stocker et al., Eds. Cambridge University Press, 867–952, doi:10.1017/CBO9781107415324.022.

Hannart, A., J. Pearl, F. E. L. Otto, P. Naveau, and M. Ghil, 2016: Causal counterfactual theory for the attribution of weather and climate-related events. *Bull. Amer. Meteor. Soc.,* **97**, 99–110, doi:10.1175/bams-d-14-00034.1.

Hansen, J., R. Ruedy, M. Sato, and K. Lo, 2010: Global surface temperature change. *Rev. Geophys.*, **48**, RG4004, doi:10.1029/2010RG000345.

IPCC, 2001: *Climate Change 2001*. J. T. Houghton et al., Eds. Cambridge University Press, 881 pp.

——, 2007: *Climate Change 2007: The Physical Science Basis*. S. Solomon et al., Eds. Cambridge University Press, 996 pp.

——, 2013: *Climate Change 2013: The Physical Science Basis. Contribution of Working Group I to the Fifth Assessment Report of the Intergovernmental Panel on Climate Change*. T. F. Stocker et al., Eds., Cambridge University Press, 1535 pp.

Kam, J., T. R. Knutson, F. Zeng, and A. T. Wittenberg, 2016: Multimodel assessment of anthropogenic influence on record global and regional warmth during 2015 [in "Explaining Extreme Events of 2015 from a Climate Perspective"]. *Bull. Amer. Meteor. Soc.*, **97** (12), S4–S8, doi:10.1175/BAMS-D-16-0138.1.

Karl, T. R., and Coauthors, 2015: Possible artifacts of data biases in the recent global surface warming hiatus. *Science,* **348**, 1469–1472, doi:10.1126/science.aaa5632.

Knutson, T. R., F. Zeng, and A. T. Wittenberg, 2013: Multimodel assessment of regional surface temperature trends: CMIP3 and CMIP5 twentieth-century simulations. *J. Climate*, **26**, 8709–8743, doi:10.1175/JCLI-D-12-00567.1.

——, T. R., R. Zhang, and L. W. Horowitz, 2016: Prospects for a prolonged slowdown in global warming in the early 21st century. *Nat. Comm.*, **7**, 13676, doi:10.1038/ncomms13676.

Lin, N., R. E. Kopp, B. P. Horton, and J. P. Donnelly, 2016: Hurricane Sandy's flood frequency increasing from year 1800 to 2100. *Proc. Nat. Acad. Sci. USA*, **113**, 12,071–12,075, doi:10.1073/pnas.1604386113.

Morice, C. P., J. J. Kennedy, N. A. Rayner, and P. D. Jones, 2012: Quantifying uncertainties in global and regional temperature change using an ensemble of observational estimates: The HadCRUT4 data set. *J. Geophys. Res.*, **117**, D08101, doi:10.1029/2011JD017187.

Stott, P. A., D. A. Stone, and M. R. Allen, 2004: Human contribution to the European heatwave of 2003. *Nature*, **432**, 610–614, doi:10.1038/nature03089.

Taylor, K. E., R. J. Stouffer, and G. A. Meehl, 2012: An overview of CMIP5 and the experimental design. *Bull. Amer. Meteor. Soc.,* **93**, 485–498, doi:10.1175/BAMS-D-00094.1.

Trenberth, K. E., J. M. Caron, D. P. Stepaniak, and S. Worley, 2002: Evolution of El Niño–Southern Oscillation and global atmospheric surface temperatures. *J. Atmos. Res.*, **107**, 4065, doi:10.1029/2000JD000298.

Table 1.1. SUMMARY of RESULTS

	ANTHROPOGENIC INFLUENCE ON EVENT		
	INCREASE	DECREASE	NOT FOUND OR UNCERTAIN
Heat	Ch. 3: Global Ch. 7: Arctic Ch. 15: France Ch. 19: Asia		
Cold		Ch. 23: China Ch. 24: China	
Heat & Dryness	Ch. 25: Thailand		
Marine Heat	Ch. 4: Central Equatorial Pacific Ch. 5: Central Equatorial Pacific Ch. 6: Pacific Northwest Ch. 8: North Pacific Ocean/Alaska Ch. 9: North Pacific Ocean/Alaska Ch. 9: Australia		Ch. 4: Eastern Equatorial Pacific
Heavy Precipitation	Ch. 20: South China Ch. 21: China (Wuhan) Ch. 22: China (Yangtze River)		Ch. 10: California (failed rains) Ch. 26: Australia Ch. 27: Australia
Frost	Ch. 29: Australia		
Winter Storm			Ch. 11: Mid-Atlantic U.S. Storm "Jonas"
Drought	Ch. 17: Southern Africa Ch. 18: Southern Africa		Ch. 13: Brazil
Atmospheric Circulation			Ch. 15: Europe
Stagnant Air			Ch. 14: Western Europe
Wildfires	Ch. 12: Canada & Australia (Vapor Pressure Deficits)		
Coral Bleaching	Ch. 5: Central Equatorial Pacific Ch. 28: Great Barrier Reef		
Ecosystem Function		Ch. 5: Central Equatorial Pacific (Chl-*a* and primary production, sea bird abundance, reef fish abundance) Ch. 18: Southern Africa (Crop Yields)	
El Niño	Ch. 18: Southern Africa		Ch. 4: Equatorial Pacific (Amplitude)
TOTAL	18	3	9

	METHOD USED		Total Events
Heat	Ch. 3: CMIP5 multimodel coupled model assessment with piCont, historicalNat, and historical forcings Ch. 7: CMIP5 multimodel coupled model assessment with piCont, historicalNat, and historical forcings Ch. 15: Flow analogues conditional on circulation types Ch. 19: MIROC-AGCM atmosphere only model conditioned on SST patterns		
Cold	Ch. 23: HadGEM3-A (GA6) atmosphere only model conditioned on SST and SIC for 2016 and data fitted to GEV distribution Ch. 24: CMIP5 multimodel coupled model assessment		
Heat & Dryness	Ch. 25: HadGEM3-A N216 Atmosphere only model conditioned on SST patterns		
Marine Heat	Ch. 4: SST observations; SGS and GEV distributions; modeling with LIM and CGCMs (NCAR CESM-LE and GFDL FLOR-FA) Ch. 5: Observational extrapolation (OISST, HadISST, ERSST v4) Ch. 6: Observational extrapolation; CMIP5 multimodel coupled model assessment Ch. 8: Observational extrapolation; CMIP5 multimodel coupled model assessment Ch. 9: Observational extrapolation; CMIP5 multimodel coupled model assessment		
Heavy Precipitation	Ch. 10: CAM5 AMIP atmosphere only model conditioned on SST patterns and CESM1 CMIP single coupled model assessment Ch. 20: Observational extrapolation; CMIP5 and CESM multimodel coupled model assessment; auto-regressive models Ch. 21: Observational extrapolation; HadGEM3-A atmosphere only model conditioned on SST patterns; CMIP5 multimodel coupled model assessment with ROF Ch. 22: Observational extrapolation, CMIP5 multimodel coupled model assessment Ch. 26: BoM seasonal forecast attribution system and seasonal forecasts Ch. 27: CMIP5 multimodel coupled model assessment		
Frost	Ch. 29: *weather@home* multimodel atmosphere only models conditioned on SST patterns; BoM seasonal forecast attribution system		
Winter Storm	Ch. 11: ECHAM5 atmosphere only model conditioned on SST patterns		
Drought	Ch. 13: Observational extrapolation; weather@home multimodel atmosphere only models conditioned on SST patterns; HadGEM3-A and CMIP5 multimodel coupled model assessent; hydrological modeling Ch. 17: Observational extrapolation; CMIP5 multimodel coupled model assessment; VIC land surface hdyrological model, optimal fingerprint method Ch. 18: Observational extrapolation; *weather@home* multimodel atmosphere only models conditioned on SSTs, CMIP5 multimodel coupled model assessment		
Atmospheric Circulation	Ch. 15: Flow analogues distances analysis conditioned on circulation types		
Stagnant Air	Ch. 14: Observational extrapolation; Multimodel atmosphere only models conditioned on SST patterns including: HadGEM3-A model; EURO-CORDEX ensemble; EC-EARTH+RACMO ensemble		
Wildfires	Ch. 12: HadAM3 atmospere only model conditioned on SSTs and SIC for 2015/16		
Coral Bleaching	Ch. 5: Observations from NOAA Pacific Reef Assessment and Monitoring Program surveys Ch. 28: CMIP5 multimodel coupled model assessment; Observations of climatic and environmental conditions (NASA GES DISC, HadCRUT4, NOAA OISSTV2)		
Ecosystem Function	Ch. 5: Observations of reef fish from NOAA Pacific Reef Assessment and Monitoring Program surveys; visual observations of seabirds from USFWS surveys. Ch. 18: Empirical yield/rainfall model		
El Niño	Ch. 4: SST observations; SGS and GEV distributions; modeling with LIM and CGCMs (NCAR CESM-LE and GFDL FLOR-FA) Ch. 18: Observational extrapolation; *weather@home* multimodel atmosphere only models conditioned on SSTs, CMIP5 multimodel coupled model assessment		
			30